The Photoassociation of 1- and 2-Acetylanthracenes with Methanol

Takashi TAMAKI

Research Institute for Polymers and Textiles, Yatabe-Higashi 1-1-4, Tsukuba, Ibaraki 305

(Received October 22, 1981)

The effect of small amounts of methanol ($\lesssim$0.34 mol dm^{-3}) upon the absorption and fluorescence spectra of 1- and 2-acetylanthracenes in hexane was investigated. While the formation of a 1 : 1 hydrogen-bonded complex in the ground state was revealed by the isosbestic points of the absorption spectra, the change in the fluorescence spectra was indicative of the photogeneration of a highly associated complex which includes at least two alcohol molecules. On the assumption that the excited 1 : 1 complex further associates with an alcohol molecule, the computer simulation by the least-squares method provided a good fit of the observed concentration dependence of methanol upon the fluorescence quantum yield. The photokinetic parameters and the thermodynamic quantities were evaluated from the simulated parameter values.

The fluorescence spectra of aromatic compounds are, in general, sensitive to solvent polarity, because the electrostatic solvent-solute interaction (dipole-dipole and dipole-induced dipole interactions) perturbs the excited singlet states of the compounds. On the other hand, the fluorescence spectra of some aromatic compounds, such as heterocycles, ketones, and amines, in nonpolar solvents are significantly affected by the addition of small amounts of a protic solvent, which are insufficient to alter the dielectric properties of the solvents.[1-4] This specific perturbation of the fluorescence is due to the formation of a hydrogen-bonded (H-bonded) complex. Recently, the photodynamics of the complex formation has been investigated by using nanosecond fluorescence spectroscopy.[5-7] In their study of time-resolved emission measurements for aminophthalimides in alcohol solvents at low temperatures, Ware and his co-workers found that the spectral shift due to the complex formation occurs in a subnanosecond, preceding the spectral shift associated with the nonspecific dipolar relaxation.[5] DeToma and Brand studied the interaction of 2-anilinonaphthalene in cyclohexane with alcohol at the ambient temperature and presented direct kinetic evidence that this system results in stoichiometric complex formation at a low alcohol concentration, followed by the reorientation of the solvent cage when the concentration of alcohol is high.[6] For the *m*-aminoacetophenone-alcohol-viscous nonpolar solvent system, Itoh and his co-workers reported the formation of an exciplex including two alcohol molecules.[7]

In a previous study of the time-dependent spectral shifts of 1- and 2-acylanthracenes in alcohols at low temperatures,[8] it was suggested that the perturbation of alcohol on the fluorescence of these compounds is caused by a combination of the specific H-bond interaction and a nonspecific dipole reorientation of the solvent, as in the case of aminophthalimide. This paper will describe the photokinetics of the complex formation for 1- (**1A**) and 2-acetylanthracenes (**2A**) with methanol in hexane.

Experimental

The acetylanthracenes (**1A** and **2A**) were the same as those used before.[8] The hexane and methanol were Spectro- and GR-grade reagents respectively and were used without further purification.

The absorption measurements were done using a Cary 17D spectrophotometer equipped with a thermostated cell holder. The concentration of the samples used was 3×10^{-5} mol dm^{-3}. Methanol was added to the sample solutions by up to 0.34 mol dm^{-3}, at which point the dielectric property of the hexane–methanol mixture solution corresponds approximately to that of dipropyl ether (ε=3.4). For the Scott plots,[9] the absorption changes in the presence of methanol were monitored by using 10-cm cylindrical cells at 440 nm for **1A** and at 424 nm for **2A**, where the absorption of uncomplexed ketones is negligible. The absorption spectra of the complex between the aromatic ketones and methanol were determined by means of the following equation:

$$\varepsilon_C(\lambda) = \varepsilon_A(\lambda)\{d(\lambda) - \alpha d_0(\lambda)\}/(1-\alpha)d_0(\lambda),$$

where $\varepsilon_A(\lambda)$ and $\varepsilon_c(\lambda)$ are the molar absorptivities of the ketones and the complex at λ nm respectively, where $d(\lambda)$ and $d_0(\lambda)$ are the absorbances in a unit of the light path at λ nm in the presence and in the absence of methanol respectively, and where α is the mole fraction of the uncomplexed ketones to the total ketones, which can be evaluated from the equilibrium constant.

The corrected fluorescence spectra were measured using a Hitachi MPF 4 spectrofluorometer. The concentrations of the samples and of methanol were the same as those used for the absorption measurements. A 1-cm square cell was placed on a thermostated cell holder connected with a Haake FK constant-temperature circulator. The excitation was done at 350 nm for **1A** and at 368 nm for **2A**, at these points the absorption spectra show their isosbestic points, so that the relative fluorescence intensities correspond directly to the relative fluorescence quantum yields. The steady-state fluorescence data were manipulated by the aid of an HP 9845B desk-top computer. Firstly, the fluorescence spectra on the wavelength scale were transformed into those on the wave-number scale, and the relative fluorescence intensities were calculated from the trapezoid rule. Secondly, the data on the fluorescence quantum yields were analyzed by the use of a software file (09845-15140) programing the nonlinear regression analysis. The initial values of the free parameters were set as 10, and the calculation was iterated until the value of each parameter converged into (1 ± 0.1) times the preceding value.

The nanosecond fluorescence measurements and the deconvolution analysis were done in ways similar to those described elsewhere.[10] Since the fluorescence lifteime of **1A** in hexane is too short ($<$1 ns) to be detected by our apparatus, no experimental result for this compound is presented.

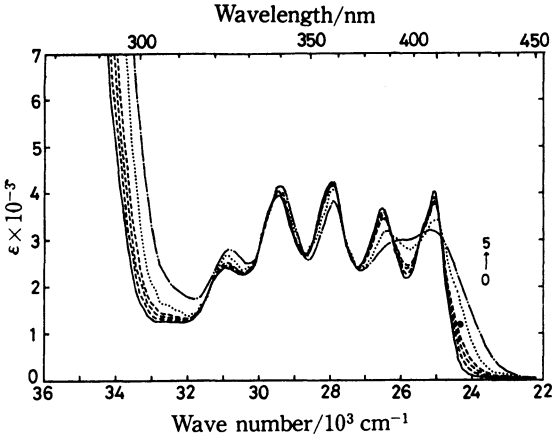

Fig. 1. Absorption spectra of 2-acetylanthracene in the binary mixture of methanol–hexane. Concentrations of methanol/mol dm^{-3}: 0) 0, 1) 0.1, 2) 0.2, 3) 0.29, 5) 24.7 (pure methanol). Spectrum 4 refers to an H-bonded complex.

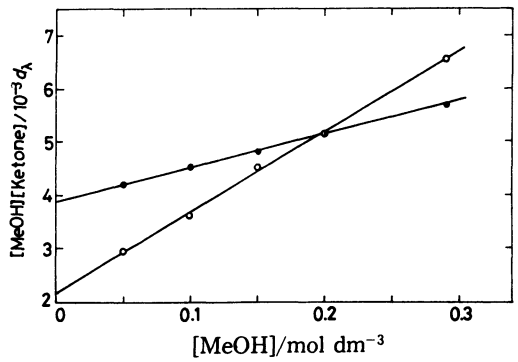

Fig. 2. Scott plots for 1- (—○—) and 2-acetylanthracene (—●—) in the binary mixture of methanol–hexane at 20 °C.

Results

The absorption spectra of **2A** in hexane in the presence and in the absence of methanol (M) are shown in Fig. 1. The apparent isosbestic points in the spectra are indicative of the formation of the complex. The Scott plots for **1A** and **2A** are shown in Fig. 2. The linearity of the plots is gratifying. The equilibrium constant (K_g) was evaluated to be 6.8 mol^{-1} dm^3 for **1A** and 2.7 mol^{-1} dm^3 for **2A** at 20 °C, only slightly dependent on the temperature. The absorption spectrum of the complex for **2A** is also shown in Fig. 1. The general form of this spectrum is close to that in pure methanol, which is also shown for the sake of comparison. The two vibrational bands lying at 376 and 388 nm in hexane are deformed, and the long wavelength edge extends to the red region. The red shift of the peak maximum amounts to *ca.* 100 cm^{-1} for **2A**. On the other hand, the spectral shift for **1A** is very small, and the peak maxima of the perturbed and unperturbed spectra are practically the same.

1A and **2A** emit a weak and structured fluorescence in hexane. The addition of small amounts of M induces a significant change in these fluorescence spectra. A

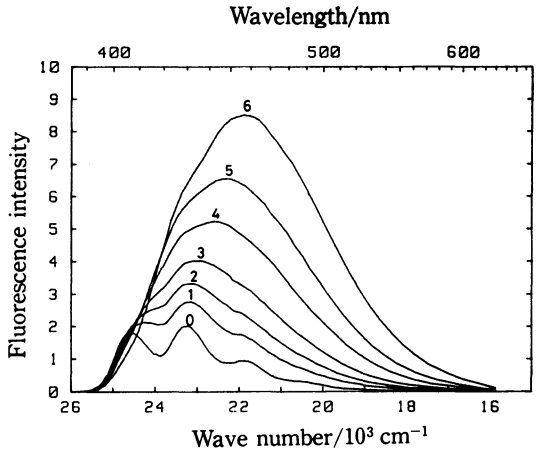

Fig. 3. Fluorescence spectra of 2-acetylanthracene in the binary mixture of methanol–hexane at 20 °C. Concentrations of methanol/mol dm^{-3}: 0) 0, 1) 0.03, 2) 0.05, 3) 0.075, 4) 0.12, 5) 0.2, 6) 0.34.

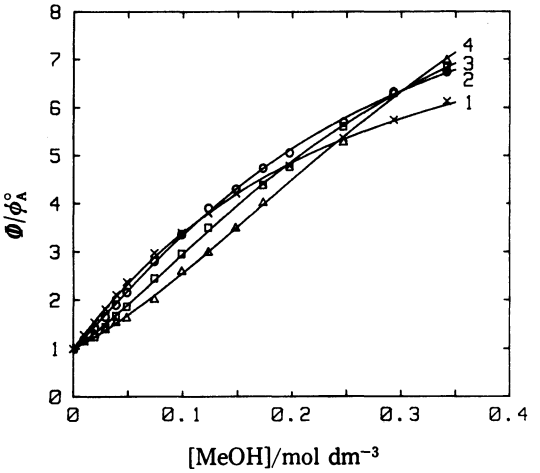

Fig. 4. Observed and simulated concentration dependence of methanol upon the relative fluorescence yield of 2-acetylanthracene. Temperature/°C: 1) 12, 2) 20, 3) 30, 4) 40.

typical example is shown in Fig. 3. The fluorescence spectra in the presence of M become intensive and move to the red area with an increase in the concentration of M ([M]). The [M] dependence of the total fluorescence quatum yield (Φ), divided by the fluorescence quantum yield (ϕ_A°) in the absence of M at several temperatures, is shown in Fig. 4.

Discussion

Reaction Scheme for the Specific Interaction of Acetylanthracenes with Methanol. The red shift of the fluorescence peak maxima for **1A** and **2A** in the presence of small amounts of M is much larger than that to be expected from the nonspecific solvent-solute interaction. As is shown in Fig. 3, the amounts of the red shift span about 30 nm under our conditions, whereas the relevent increase in the solvent polarity causes the fluorescence spectra of **1A** and **2A** to shift toward the red region by only several nm. Therefore, it appears probable that

the observed change in the fluorescence spectra is mainly due to the specific interaction between the aromatic ketones and M. The effect of added M on the fluorescence spectra is not only the red shift of the peak maxima, but also the broadening of the bandwidth, indicating the appearance of the emission band which can be ascribed to the H-bonded complex. Furthermore, the fluorescence spectra for **2A** show that an isoemissive point near 410 nm does not come out until [M] reaches *ca.* 0.05 mol dm^{-3}. This suggests that a highly associated complex, that is, one in which at least two alcohol molecules are intimately associated with the aromatic ketone, is photogenerated at a relatively high [M].

Consequently, the following reaction scheme can be postulated for the specific interaction of **1A** and **2A** with M:

$$A \underset{-M}{\overset{+M,\,K_g}{\rightleftharpoons}} C, \tag{1}$$

$$A \xrightarrow{h\nu} A^*, \tag{2}$$

$$C \xrightarrow{h\nu} C^*, \tag{3}$$

$$A^* \underset{-M,\,k_4}{\overset{+M,\,k_3}{\rightleftharpoons}} C^* \underset{-M,\,k_8}{\overset{+M,\,k_7}{\rightleftharpoons}} E^* \qquad (k_1,\ k_2;\ k_5,\ k_6;\ k_9,\ k_{10}) \tag{4}$$

$$A + h\nu'\ A \quad C + h\nu''\ C \quad C + M + h\nu'''\ C + M,$$

where A is the uncomplexed ketones, where C and E are the complexes including one and two alcohol molecules respectively, where the superscript asterisk represents the excited singlet state, and where the k's are the rate constants of the respective processes.

There is a possibility that the more highly associated complexes other than E are successively photogenerated at a high [M]. However, such a situation, requiring more sophisticated kinetic treatments, is not considered in this work. In fact, the fluorescence data observed are well consistent with the reaction kinetics to be described below.

Kinetic Treatments for Steady-state Fluorescence. In the photostationary state, the fluorescence quantum yields (ϕ) of A, C, and E relative to $\phi_A^\circ = k_1/(k_1+k_2)$ are given by the following equations:

$$\phi_A/\phi_A^\circ = \frac{\{1+P_3(1+P_1[M])+P_6[M]\}}{(\text{Denominator})}, \tag{5}$$

$$\phi_C/\phi_A^\circ = \frac{P_4[M]\{P_1+P_2(1+P_1[M])\}}{(\text{Denominator})}, \tag{6}$$

$$\phi_E/\phi_A^\circ = P_5[M](\phi_C/\phi_A^\circ), \tag{7}$$

where the ϕ's are defined as $\phi_A = k_1[A^*]/\{\varepsilon_A(\lambda)[A]+\varepsilon_C(\lambda)[C]\}$ *etc.*, (Denominator)$=(1+P_1[M])\{(1+P_2[M])\times(1+P_6[M])+P_3\}$, and

$$P_1 = K_g\varepsilon_C(\lambda)/\varepsilon_A(\lambda),$$
$$P_2 = k_3/(k_1+k_2),$$
$$P_3 = k_4/(k_5+k_6),$$
$$P_4 = k_5(k_1+k_2)/k_1(k_5+k_6),$$
$$P_5 = k_7k_9/k_5(k_8+k_9+k_{10}),$$
$$P_6 = k_7(k_9+k_{10})/(k_5+k_6)(k_8+k_9+k_{10}).$$

If these three fluorescence quantum yields could be separately determined, it would be possible to ascertain whether or not the parameter values evaluated from these experimental runs were consistent with each other. Previously, we tried to divide the perturbed fluorescence spectra into the component spectra arising from the uncomplexed ketone and the complex by subtracting the unperturbed spectra from the perturbed spectra, those which were normalized on the short wavelength side where the contribution of the complex is negligible.[8] This technique is, however, not practical in quantitative kinetic treatments, for the low fluorescence intensity at the normalized wavelength makes the errors in the subtraction procedure considerable. Moreover, it can not be applied to the **1A**–M system, for the fluorescence intensities, even on the short-wavelength side, show a monotonous increase with an increase in [M], presumably because of the large overlapping of the component spectra. Therefore, we directly analyzed the data observed for Φ/ϕ_A°, which should conform to this equation:

$$\Phi/\phi_A^\circ = 1 + [M]\{P_4(1+P_5[M]) - (1+P_6[M])\}\times \{P_1+P_2(1+P_1[M])\}/(\text{Denominator}). \tag{8}$$

Since P_1 can be independently determined from the absorption measurements, the fitting of the plots by the nonlinear regression analysis was done by holding P_1 fixed and by treating the others (P_2—P_6) as free parameters. The results for the computer simulation are shown in Fig. 4, while the values of the parameters obtained are listed in Table 1. Although the apparent dependencies of [M] on Φ/ϕ_A° are different from temper-

Table 1. Calculated parameter values

Temperature °C	P_1	P_2	P_3	P_4	P_5	P_6	SSR[a]
			1-Acetylanthracene				
12	6.8	11.1	3.0	10.5	4.0	0.6	0.087
20	6.7	10.7	4.8	11.4	5.0	0.7	0.16
30	6.6	8.6	7.0	11.4	8.6	2.3	0.037
40	6.5	5.7	10.1	11.0	12.6	4.7	0.038
			2-Acetylanthracene				
12	2.7	2.1	0.5	10.7	5.8	7.6	0.023
20	2.7	4.9	1.7	9.2	7.5	7.2	0.029
30	2.6	6.8	4.3	9.5	8.6	7.6	0.027
40	2.6	9.8	11.3	12.2	6.8	5.6	0.044

a) Sum of squared residuals.

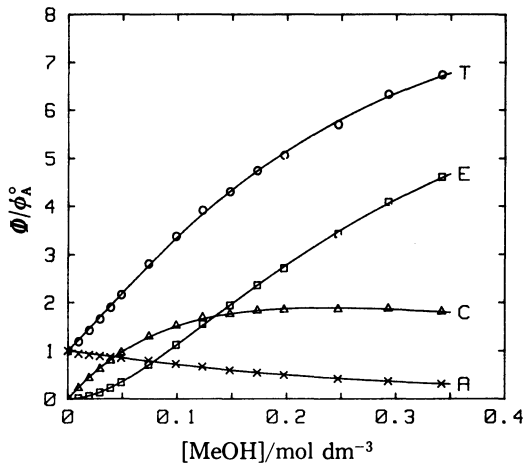

Fig. 5. Simulated concentration dependence of methanol upon the relative fluorescence yield of three emissive components for 2-acetylanthracene: A) an uncomplexed ketone, C) a 1 : 1 complex, E) a 1 : 2 complex, T) A+C+E.

ature to temperature, the simulated curves satisfactorily smooth the observed plots with the order of 10^{-2} of the sum of the squared residuals for all the experimental runs. This strongly supports the validity of the reaction scheme postulated. Particularly, the sigmoid and upward dependencies of [M] revealed at relatively high temperatures are characteristic of the formation of a highly associated complex; the formation of C alone results in no such dependencies.

The functions $\{\phi_A([M])/\phi_A^\circ$, *etc.*$\}$ predicted from Eqs. 5—7 for **2A** at 20 °C are shown in Fig. 5. It can be seen that, as [M] increases, ϕ_A decreases; ϕ_C, which increases at first, decreases slightly, and ϕ_E increases at the expense of ϕ_C. On the assumption that the only emissive species at very low [M] values are A and C, and that the peak maxima and the forms of these two fluorescence spectra do not change at higher [M] values, the perturbed fluorescence spectra can be divided into their three component spectra by using the predicted fluorescence quantum yields. The fluorescence spectra of E thus obtained were found to be invariant in general form and peak maximum at [M]$\leqslant$0.25 mol dm^{-3}. An example of such a spectral division for **2A** at [M]=0.12 mol dm^{-3} at 20 °C is shown in Fig. 6. The fluorescence spectra of the H-bonded complexes (C and E) become structureless and move to the red with an increase in the number of the associated alcohol molecule. The energies of the fluorescence peak maxima of A, C, and E for **1A** and **2A** at 20 °C, together with the amounts of the red shift relative to A, are listed in Table 2.

Photokinetics for Pulse Excitation at Low [M]. At low [M] values, where the perturbed fluorescence spectra consist of A and C, the contribution of E being negligible, the observed time evolution of the fluorescence is the convolution of a lamp decay profile, with the true fluorescence decay function given in this form:

$$F(t) = C_1 \exp(-\lambda_1 t) + C_2 \exp(-\lambda_2 t) \quad (9)$$

where:

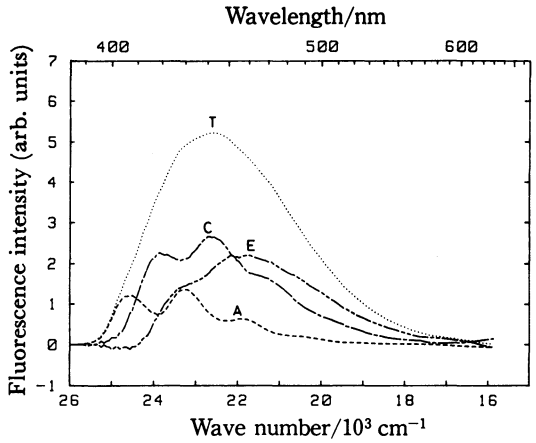

Fig. 6. Division of the fluorescence spectrum of 2-acetylanthracene in the presence of methanol (0.12 mol dm^{-3}) into three component spectra: T) the fluorescence spectrum as observed, A) an uncomplexed ketone, C) a 1 : 1 complex, E) a 1 : 2 complex.

TABLE 2. FLUORESCENCE PEAK MAXIMA OF THE UNCOMPLEXED KETONE (A), 1 : 1 COMPLEX (C), AND 1 : 2 COMPLEX (E)

Compound	λ_A/nm	λ_C/nm ($\Delta\tilde{\nu}_{A-C}$/cm^{-1})[a]	λ_E/nm ($\Delta\tilde{\nu}_{A-E}$/cm^{-1})[a]
1-Acetylanthracene	449	465	483
		(767)	(1568)
2-Acetylanthracene	431	440	460
		(475)	(1463)

a) The amounts of the red shift relative to A.

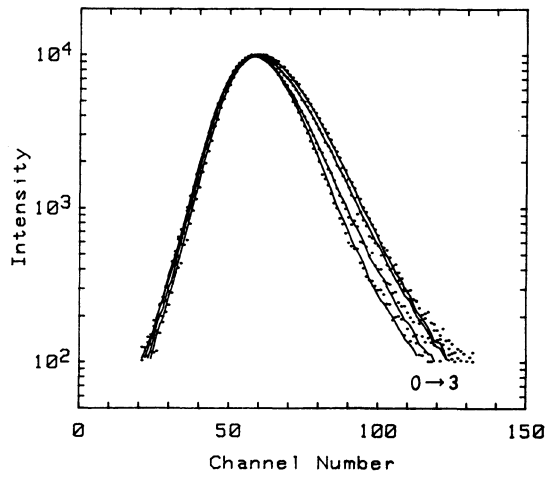

Fig. 7. Observed and simulated time evolution of the fluorescence of 2-acetylanthracene in the binary mixture of methanol–hexane at 20 °C. Concentrations of methanol/mol dm^{-3}: 0) 0, 1) 0.01, 2) 0.03, 3) 0.05.

$$\lambda_{1,2} = (1/2)(k_1 + k_2 + k_3[M] + k_4 + k_5 + k_6) \pm \sqrt{(k_1+k_2+k_3[M]-k_4-k_5-k_6)^2+4k_3k_4[M]},$$

and:

$$\lambda_1 + \lambda_2 = k_1 + k_2 + k_3[M] + k_4 + k_5 + k_6, \quad (10)$$

$$\lambda_1\lambda_2 = (k_1 + k_2)(k_4 + k_5 + k_6) + k_3(k_5 + k_6)[M]. \quad (11)$$

The related photokinetics for the time evolution of the

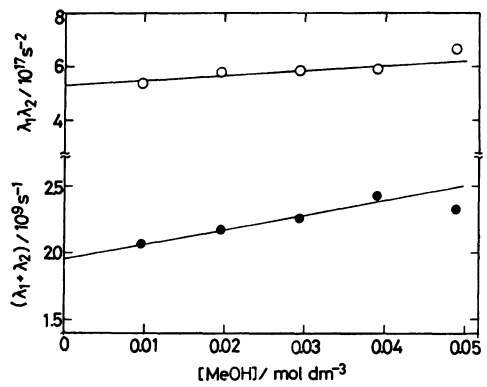

Fig. 8. Plots of $\lambda_1+\lambda_2$ and $\lambda_1\lambda_2$ *vs.* [methanol] for 2-acetylanthracene.

fluorescence at high [M] values remains unresolved in this paper, since the luminescent system involving ternary components makes the kinetic analysis extremely complex.

Figure 7 shows the actual time evolution of the fluorescence monitored at 430 nm for **2A** in the presence of M ($\leqslant$0.05 mol dm^{-3}) at 20 °C, together with the decay curves calculated by the method of convolution, assuming Eq. 9. The observed decay curves are well simulated by the biexponential decay function. The plots for $\lambda_1+\lambda_2$ and $\lambda_1\lambda_2$ *vs.* [M] are shown in Fig. 8. From the slopes of these two linear plots, the values of k_3 and k_5+k_6 are obtained as 1.1×10^{10} mol^{-1} dm^3 s^{-1} and 1.8×10^8 s^{-1} respectively. The intercepts of these plots at [M]=0 give $k_1+k_2+k_4+k_5+k_6=1.9\times10^9$ s^{-1} and $(k_1+k_2)(k_4+k_5+k_6)=5.4\times10^{17}$ s^{-1}, yielding $k_1+k_2=1.6\times10^9$ s^{-1} and $k_4+k_5+k_6=3.4\times10^8$ s^{-1}; the value of k_1+k_2 is within the limits of experimental error, proximate to the reciprocal of the fluorescence lifetime independently measured for **2A** in the absence of M at 20 °C ($1/\tau_A^\circ=1/(k_1+k_2)=1.4\times10^9$ s^{-1}). The values of the other rate constants (k_3—k_6) are in line with those evaluated from the steady-state measurements, as will be described below.

Evaluation of Photokinetic Parameters. By analogy with ϕ_A° and τ_A°, the intrinsic fluorescence efficiencies (ϕ°) and lifetimes (τ°) for C and E are written as follows; $\phi_C^\circ=k_5/(k_5+k_6)$, $\tau_C^\circ=1/(k_5+k_6)$, $\phi_E^\circ=k_9/(k_9+k_{10})$, and $\tau_E^\circ=1/(k_9+k_{10})$. One can derive the following equations;

$$\phi_C^\circ/\phi_A^\circ = (k_5/k_1)(\tau_C^\circ/\tau_A^\circ) = P_4, \quad (12)$$

$$\phi_E^\circ/\phi_A^\circ = (k_9/k_1)(\tau_E^\circ/\tau_A^\circ) = P_4P_5/P_6. \quad (13)$$

The parameter values on the right-hand side of these equations (P_4 and P_4P_5/P_6) were evaluated to be in the order of 10 (Table 1), indicating that ϕ_C° and ϕ_E° are an order of magnitude greater than ϕ_A°. The low ϕ_A° values for **1A** and **2A** are mainly due to an intersystem crossing to an upper triplet state lying near the singler state.[10] The fluorescence intensity of acylanthracenes involving **1A** and **2A** is sensitive to external variables, which induce the displacement of the excited singlet level, such as the solvent polarity,[10] the temperature,[8] and the pressure.[11] It generally increases with a decrease in the excited singlet level, which is interpreted as a result of the inhibition of the intersystem crossing due to the increase in the energy separating the singlet and triplet levels.[12] From the fact that the fluorescence spectra of C and E are sufficiently red-shifted (Fig. 6 and Table 2), the fluorescence enhancement due to the H-bond interaction may be explained by a related mechanism. This would require a decrease in the nonradiative rate constant (k_6, $k_{10}\ll k_2$). On the other hand, the alternative possibility that the increase in the radiative rate constant plays a role can be excluded for the following reasons: (1) $\tau_C^\circ/\tau_A^\circ$ for **2A** at 20 °C was obtained from the pulse-excitation measurements to be 8.9, a value which agrees well with that of P_4 (Table 1). This immediately leads to $k_5/k_1\simeq1$; *i.e.*, the radiative rate constants of A and C are almost the same. (2) This consequence is also suggested by the close simmilarity between the oscillator strengths calculated from the long-wavelength absorption bands of these emissive species (Fig. 1). With these points in mind, it appears likely that k_5 and, presumably, k_9 are approximately equal to k_1, though no specific information about k_9 was obtained.

The values of ϕ_C° and ϕ_E° were evaluated from the observed ϕ_A° values, and, on the assumption of $k_1\simeq k_5\simeq k_9$, the values of τ_C° and τ_E° were obtained from the observed τ_A° values. The results for **2A** are listed in Table 3. The values of k's except k_7 and k_8, to which there is no satisfactory route, were determined as follows; the radiative rate constants (k_1, k_5, and k_9) from the corresponding ϕ° and τ° values, the nonradiative rate constants (k_2, k_6, and k_{10}) from the corresponding $1-\phi^\circ$ and τ° values, k_3 from P_2 and τ_A°, and k_4 from P_3 and τ_C°. The results for **2A** are also listed in Table 3. The values of k_3, k_4, and k_5+k_6 at 20 °C are comparable with the

Table 3. Fluorescence efficiencies (ϕ°) and lifetimes (τ°) of the uncomplexed (A), 1 : 1 complex (C), and 1 : 2 complex (E), and rate constants for 2-acetylanthracene

Temp/°C	ϕ_A°	τ_A°/ns			ϕ_C°	τ_C°/ns	ϕ_E°	τ_E°/ns
12	0.023	0.91			0.25	9.7	0.19	7.4
20	0.020	0.73			0.18	6.7	0.19	7.0
30	0.018	0.68			0.17	6.5	0.19	7.3
40	0.016	0.57			0.20	7.0	0.24	8.4
	$k_1/10^7$ s^{-1}	$k_2/10^8$ s^{-1}	$k_3/10^9$ M^{-1} s^{-1}	$k_4/10^8$ s^{-1}	$k_5/10^7$ s^{-1}	$k_6/10^8$ s^{-1}	$k_9/10^7$ s^{-1}	$k_{10}/10^8$ s^{-1}
12	2.5	11	2.3	0.51	2.5	0.8	2.5	1.1
20	2.7	13	6.7	2.5	2.7	1.2	2.7	1.2
30	2.7	14	10	6.7	2.7	1.3	2.7	1.1
40	2.8	17	17	16	2.8	1.2	2.8	0.9

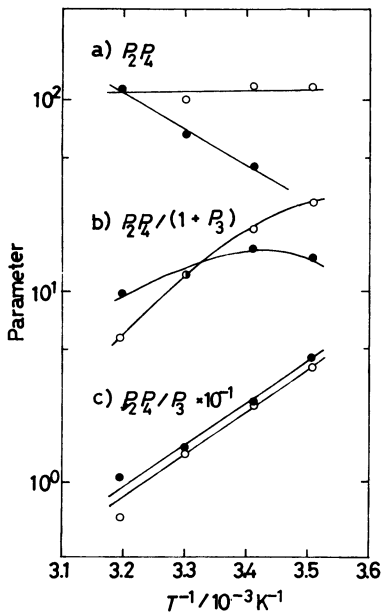

Fig. 9. Temperature dependence of a) $\log P_2P_4$, b) $\log P_2P_4/(1+P_3)$, and c) $\log P_2P_4/P_3$, for 1-(—○—) and2-acetylanthracene (—●—).

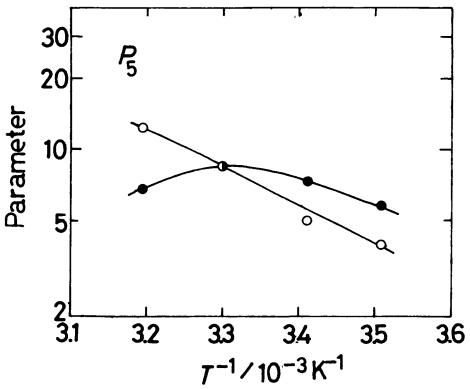

Fig. 10. Plots of $\log P_5$ *vs.* T^{-1} for 1-(—○—) and 2-acetylanthracene (—●—).

respective values determined independently from the pulse-excitation measurements at the same temperature.

The thermodynamic quantities associated with the complex formation in the excited state were determined by using the following equations:

$$\log P_2P_4/(1+P_3) \simeq \log k_3\tau_C^\circ/(1+k_4\tau_C^\circ), \quad (14)$$

$$\log P_5 \simeq \log k_7\tau_E^\circ/(1+k_8\tau_E^\circ), \quad (15)$$

where $k_1 \simeq k_5 \simeq k_9$ is assumed. The experimental curves of the left-hand sides in Eqs. 14 and 15 against T^{-1} (T: absolute temperature) are plotted in Figs. 9b and 10 respectively. The slopes of these curves are negative and/or positive with respect to T. In the case of Fig. 9b, the negative temperature dependence is realized when $k_4\tau_C^\circ$ $(=P_3)>1$. Eventually, Eq. 14 can be reduced to this equation; $\log P_2P_4/P_3 \simeq \log k_3/k_4$, suggesting that the limiting temperature coefficient is consistent with the slope of the plots for $\log P_2P_4/P_3$, which can be ascribed to the enthalpy change (ΔH_C°) for the photoassociation of C. From the linear relationship obtained for $\log P_2P_4/P_3$ *vs.* T^{-1} (Fig. 9c), the value of ΔH_C° was found to be -9 kcal mol^{-1} for **1A** as well as for **2A**. The ΔH_C° values estimated from the extrapolation of the slopes shown in Fig. 9b agreed with this value within ± 2 kcal mol^{-1}. The entropy change (ΔS_C°) was calculated as -26 cal deg^{-1} mol^{-1} for **1A** and as -24 cal deg^{-1} mol^{-1} for **2A**, suggesting a rather rigid and tight complex. On the other hand, it appears likely that $k_4\tau_C^\circ$ $(=P_3)<1$ holds for the positive slope of the plots for $\log P_2P_4/(1+P_3)$, though there are few data on this side. At this time, Eq. 14 can be rewritten as $\log P_2P_4 \simeq \log k_3\tau_C^\circ$, suggesting that a thermally activated process (k_3) is responsible for the positive temperature dependence. The plots of $\log P_2P_4$ *vs.* T^{-1} are shown in Fig. 9a. The temperature coefficient for **2A** was found to be about 8 kcal mol^{-1}, ascribable to the activation energy for k_3 (ΔE_3), since τ_C° is little dependent on T (Table 3). The value of ΔE_3 obtained is larger than that to be expected from a diffusion-controlled reaction in hexane (*ca.* 2 kcal mol^{-1} [13]). The curve for **1A** is practically temperature-independent; this may be due to the fact that the negative temperature dependence of τ_C° cancels out the positive temperature dependence of k_3, but the details remain uncertain.

In substantially similar ways, the results shown in Fig. 10 can be analyzed to give the enthalpy change (ΔH_E°) and the activation energy (ΔE_7) associated with the formation of E. The plots of $\log P_5$ *vs.* T^{-1} for **2A** give the curve with $\Delta H_E^\circ \simeq -10$ kcal mol^{-1} at low temperatures and with $\Delta E_7 \simeq 5$ kcal mol^{-1} at high temperatures (the evaluation of these values is only approximate, because there are few data on either side). From the curve for **1A**, which has a positive slope over the temperature range employed, the value of ΔE_7 was evaluated to be 7 kcal mol^{-1} on the assumption that τ_E° is temperature-independent.

Conclusively, the fluorescence change observed can be explained as stoichiometric complex formation in the ground and excited states. It is striking that the steady-state fluorescence data are well simulated by the highly-associated-complex model. In the study of the time-resolved fluorescence measurements for *m*-aminoacetophenone–alcohol–viscous nonpolar solvent systems, Itoh and his co-workers observed the time-dependent fluorescence shift associated with the formation of E.[7] In contrast with their observations, no time-dependent spectral shift could be detected in the present cases using our detecting system. However, this is not necessarily in contradiction with our model, because it appears likely that, under the present experimental conditions, the relaxation by the H-bond interaction is so rapid that the time-resolved fluorescence observed is distorted by the convolution of the light pulse, which has a definite duration (half bandwidth $\simeq 6$ ns), with the decay of the sample.

On the other hand, time-resolved fluorescence measurements in viscous alcohol at low temperatures are informative from the viewpoint of complex formation. It was shown that the fluorescence spectrum of **2A** in propylene glycol undergoes time-dependent changes even at -125 °C, where the solvent relaxation time is much slower than the fluorescence decay time. This

spectral change may be ascribed to the specific solvent-solute interaction, since a general solvent relaxation would induce a more drastic change in the fluorescence spectrum of this compound.[8] Moreover, the fluorescence spectra monitored at zero- and several-ten-ns delay times at −125 °C (*cf.* Fig. 4 in Ref. 8) are quite similar to those of C and E respectively (Fig. 4). These results may support the conclusion reached in this study.

It appears probable that the complex formation is facilitated in the excited state, since the photoexcitation leads to preferential electron migration from the anthryl ring to the carbonyl group, resulting in an increase in the carbonyl basicity.[8] Therefore, the formation of the highly associated complex is electronically reasonable, but the conformation of this complex remains uncertain at this stage of the investigation.

References

1) N. Mataga and S. Tsuno, *Bull. Chem. Soc. Jpn.*, **30**, 368 (1957).
2) H. Kokubun, *Z. Phys. Chem. N. F.*, **17**, 281 (1958); **101**, 137 (1976).
3) K. Bredereck, Th. Förster, and H.-G. Oesterlin, "Luminescence of Organic and Inorganic Materials," ed by H. P. Kallmann and G. M. Spruch, John Wiley and Sons, New York (1962), p. 161.
4) M. Kitamura and H. Baba, *Bull. Chem. Soc. Jpn.*, **48**, 1191 (1975).
5) W. R. Ware, S. K. Lee, G. J. Brant, and P. P. Chow, *J. Chem. Phys.*, **54**, 4729 (1971).
6) R. P. DeToma and L. Brand, *Chem. Phys. Lett.*, **47**, 231 (1977).
7) Y. Tanimoto, K. Inoue, Y. Furukawa, Y. Segawa, and M. Itoh, *Bull. Chem. Soc. Jpn.*, **52**, 1601 (1979).
8) T. Tamaki, *Bull. Chem. Soc. Jpn.*, **53**, 577 (1980).
9) R. L. Scott, *Rec. Trav. Chim.*, **75**, 787 (1956).
10) T. Tamaki, *Bull. Chem. Soc. Jpn.*, **55**, 1756(1982).
11) D. J. Mitchell, G. B. Schuster, and H. B. Drickamer, *J. Am. Chem. Soc.*, **99**, 1145 (1977).
12) S. Hirayama, *Rev. Phys. Chem. Jpn.*, **42**, 49 (1972).
13) J. B. Birks, M. D. Lumb, and I. H. Munro, *Proc. R. Soc. London, Ser. A*, **280**, 289 (1964).